Revue du CAMES – Sciences Appliquées et de l'Ingénieur
Cames 2017 - *Published Online 2017* - http://publication.lecames.org/
Vol. 2(1), pp. 13-21, Online July 2017

Vol. 2(1)
ISSN 2312-8712
June 2017

Full Length Research Paper

Characterization of silicon carbon nitride thin films synthesised by continuous micro-wave plasma assisted chemical vapour deposition

P. Kouakou[1], P. Yoboué[2], B. Ouattara[1], M. Belmahi[3]

[1] Laboratoire de Physique Fondamentale et Appliquée, UFR Sciences Fondamentales et Appliquées, Université Nangui Abrogoua, 02 BP 801 Abidjan 02, Côte d'Ivoire
[2] Ecole Supérieure Africaine des Technologies de l'Information et de la Communication (ESATIC), Abidjan, Côte d'Ivoire
[3] Institut Jean Lamour (IJL) CNRS UMR 7198, Université de Lorraine, Faculté des Sciences et Technologies, BP 239, F-54506 Vandoeuvre Cedex, France

Received January 2017 – Accepted March 2017

**Corresponding author. E-mail: ahoutoupaul@gmail.com*
Author(s) agree that this article remain permanently open access under the terms of the Creative Commons Attribution License 4.0 International License.

Abstract:
Crystalline silicon carbon nitrite thin films have been synthesized by continuous MPACVD in N_2/CH_4 gas mixture on silicon substrates. Prior deposition, discharges stabilisations have been studied and then the plasma is analysed in-situ by optical emission spectroscopy according to experimental parameters (microwave power, gas mixture, pressure and flow rate). Several techniques have been used to characterize the films. Morphological analyses realized by SEM, TEM and AFM show that the films are nano-crystalline and their roughness is around 5 nm. The XRD spectrum and selected area electron diffraction patterns exhibit a signature that correspond to beta-C_3N_4 and SiCN. EDXS and XPS analyses show the presence of C, N, Si and O. The C1s, N1s and Si2p levels obtained from XPS confirm the presence of C-N, Si-C and Si-N covalent bonds typical for SiCN and CN_x films. The presence of Si is justified by the participation of the substrate to the growth by etching. The oxygen comes from the exposure of the films to atmosphere after deposition. The surface was not cleaned by argon bombardment to avoid a structural and bonding modification of the film.

Keyword: Silicon carbon nitride, Microwave plasma CVD, Surface characterization, hard film coatings, CNx.

Cite this article:
P. Kouakou, P. Yoboué, B. Ouattara, M. Belmahi (2017). Characterization of silicon carbon nitride thin films synthesised by continuous micro-wave plasma assisted chemical vapour deposition. Revue Cames – Sci. Appl. & de l'Ing., Vol. 2(1), pp. 13-21. ISSN 2312-8712.

Acronyms

MPACVD	Microwave Plasma Assisted Chemical Vapour Deposition
SEM	Scanning Electron Microscopy
TEM	Transmission Electron Microscopy
AFM	Atomic Force Microscopy
EDXS	Energy Dispersion X-ray Spectroscopy
XPS	X-ray Photoelectrons Spectroscopy

1. Introduction

In 1989 Liu and Cohen predicted that the β-C_3N_4 would exhibit properties close to those of diamond [1], enabling many applications, for instance in mechanics due to their hardness and in medicine [2] due to their low friction coefficient. The predicted hardness of the β-C_3N_4 around 427 GPa is close to that of natural diamond (443 GPa). It could so be used especially as a protective layer against corrosion, oxidation, stripe, wear, and fatigue. Since this study, many deposition techniques are used to attempt the carbon nitride materials synthesis, namely: ion beam deposition techniques or plasma based techniques such as Pulsed Laser Deposition (PLD) [3, 4], Electron Cyclotron Resonance (ECR) [5, 6], Direct Current (DC) or Radio Frequency (RF) [7, 8], Inductively Coupled Plasma Chemical Vapor Deposition (ICP-CVD) [9], Microwave Plasma Assisted Chemical Vapor Deposition (MPACVD) [10-12].

At this time, nobody has already attended the synthesis of a mono-phase β-C_3N_4. For most of the works, the results show an impossibility to control the films

phases, their stoichiometry and especially their nitrogen content.
Several reviews comparing these techniques of synthesis and the characterization of the resulting films were published [13-15]. Some of them make critical comments on the advantages and drawbacks of the elaboration techniques. Indeed, at this time, doubt still exists whether β-C_3N_4 can be obtained or not, insofar as nobody has reached the synthesis of pure β-C_3N_4 thin film. At best the crystalline β-C_3N_4 phase was obtained in very small proportions and was always embedded in other phases like α-C_3N_4, c-C_3N_4, graphitic C_3N_4, amorphous CN_x or crystalline SiCN.
MPACVD is a very powerful technique, which is frequently and successfully used to synthesise diamond in H_2/CH_4 gas mixture [16]. Unfortunately, polycrystalline diamond deposits do not meet all industrial requirements for mechanical applications because of fragility and delaminating problems. There is still good hope that CN_x polycrystalline films, which could be at least as hard as diamond will solve these problems. The MPACVD technique gives excellent results for good quality diamond synthesis, and was naturally tested for the CNx growth in this study. This technique is the most used in literature to obtain crystalline CNx phases thanks to the high gas temperature and dissociation rates, as it has been proved for diamond synthesis [10-12, 17].
In this work, the evolution of the intensity of the species present in the N_2/CH_4 continuous microwave plasma is studied by Optical Emission Spectroscopy (OES) as a function of the of the CH_4 percentage in the gas mixture. The Films are then realized as a function of the plasma parameters and characterized by combining different techniques. The morphology, the structure and the chemical composition of the obtained films are studied. The results from these complementary techniques lead to discuss on the different phases present in the films. The characterisation of carbon nitride thin films, particularly the identification of the β-C_3N_4 phase is very complicate due to the poor bibliography on the subject and the controversial interpretation encountered in the literature. The work of Malkov [18] summarizes this problem. We proposed combination of SAED and XRD methods to identify the phases present in the film.

2. Experimental process

The growth of carbon nitride thin films is carried out in a MPACVD reactor that was described in details by Lamara et al [16]. Briefly, a mixture of gas is introduced into a chamber and the molecules are dissociated by a microwave (2.45 GHz) injected in the chamber through a waveguide. The gas mixture is composed by N_2 and CH_4. The substrate is a 2 cm^2 B doped Si (100). Prior to be introduce in the chamber of the reactor, the substrates are cleaned with different solvents. The principal deposition parameters are: the microwave power, the gas pressure, the total gas flow and the gas percentages. The plasma is studded as a function of the different parameters by optical emission spectroscopy with a Jobin Yvon 550 TRIAX monochromatic spectrometer with a CCD detector. The growth duration for all the films is 8 h. In this study, the CH_4 percentage is fixed at 4% for the films realization in order to avoid carbon balls formation at the films surface as it has been observed in a previous work [19]. The substrate temperature measured by an infra-red pyrometer is around 900°C. Scanning Electron Microscopy (SEM) observations are performed on a JEOL JSM-6500F using an accelerating voltage of 5 kV to analyse the general morphology of the films. The surface roughness is analysed by Atomic Force Microscopy (AFM). The Transmission Electron Microscopy (TEM) is used to deepen the knowledge on the crystallites size and morphology. TEM observations are carried out on a Philips CM20 microscope operating at an accelerating voltage of 200 kV. They are performed on matter chips sampled on the films by the micro cleavage technique. During TEM imaging, some samples of Selected Area Electronic Diffraction (SAED) measurements were performed. X-ray Photoelectrons Spectroscopy (XPS) analyses are also done in order to determine the bonding structure and the surface chemical composition. The XPS spectra were obtained by a multi-detection analyzer (VSW CL150 in fixed analyser transmission mode). The unmonochromatized Mg Kα (1253.6 eV) source operated at 15 kV and 10 mA. The pressure in the analytical chamber was 10^{-7} Pa. The resolution is lower than 1 eV. The charge effects were corrected using Ag3d5/2 at 368.2 eV [20]. The recorded lines (Si2p, N1s, C1s, and O1s) were fitted using a curve-fitting program with Gaussian–Lorentzian (XPSpeak4.1).
The crystallographic structure is determined by X-ray diffraction (XRD). The θ-2θ XRD patterns are performed on a Philips X'PERT PRO apparatus (Cu K_α radiation, λ=1.54056 Å).

3. Results and discussion

Prior to this study, it's necessary to be sure that the plasma is stable in the chamber of the reactor and in the time during the deposition.

1. - Plasma stabilization

Before the realization of the films, we have identified the different species present in the plasma and study they evolution while varying the plasma parameters in order to know later, they influence on the obtained films. For this study, the stabilization of the plasma is very important for long duration films deposition. Indeed, during the deposition, the plasma must keep constant its morphology and position in the chamber of the reactor. The plasma is so hot that its contact with the quartz window can produce damages. The morphology and the position of the plasma depend on the plasma parameters. The **Erreur ! Source du renvoi introuvable.** shows an example of these morphological and spatial variations of the plasma according to the gas pressure.

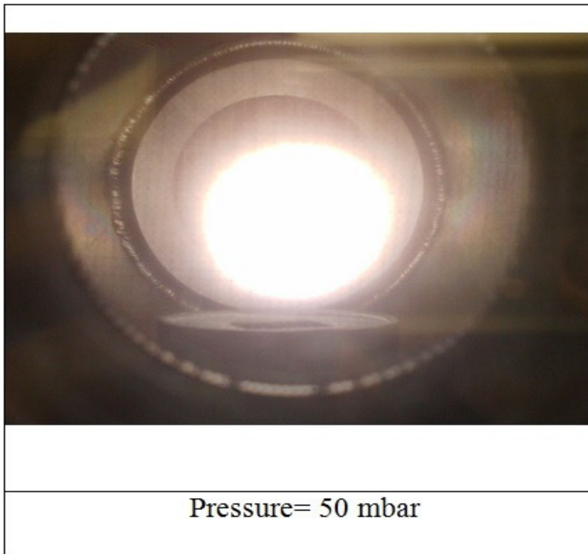

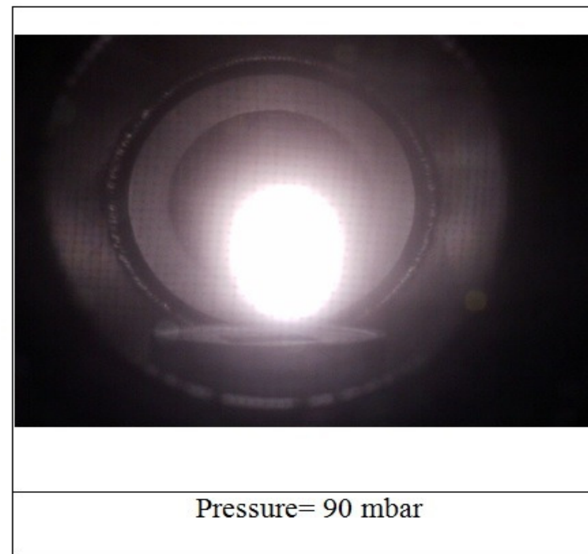

Figure 1. Morphology and spatial position of a typical plasma in the reactor chamber by varying the gas pressure, same gas mixture N_2/CH_4 4% and same micro-wave power= 1000 W

This figure shows for example that by changing the gas pressure, the plasma goes up or down. The volume of the plasma can increase or decrease until the plasma turn of. When methane is injected in the nitrogen plasma for example, the plasma become more stable than pure N_2 plasma, but when the pressure or the micro-wave power is increased, it becomes instable again. Taking account these problems, the plasma parameters have been delimitated. That permits to make the experiments possible in our reactor as shown in **Erreur ! Source du renvoi introuvable.**.

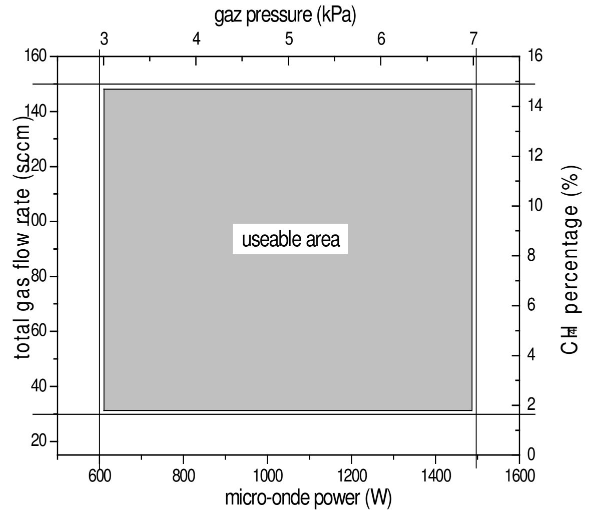

Figure 2. Plasma stabilization zone as a function of the gas pressure, the gas flow rate, the CH_4 percentage and the microwave power that permit to obtain stable plasma for film deposition

On the **Erreur ! Source du renvoi introuvable.** the area in the middle corresponds to the delimitated parameters that are really usable to obtain stable plasma for long duration deposition. The plasma power should be increased if the gas pressure increases. Indeed, increasing the gas pressure means decreasing the electrons mean free path. That breeds a diminution of the plasma volume and a possible extinction of the plasma if the microwave power is not increased. Otherwise, when the percentage of the methane increases, the plasma temperature increases. This is due to the formation of exothermic carbonate radicals such as CN. To keep the plasma temperature constant, it is necessary to increase the gas flow rate to pump exothermic radicals and renew the gaz.

2. - Plasma diagnostic by optical emission spectroscopy

The Optical Emission Spectroscopy (OES) has been described elsewhere in our previous work [19]. It is a technique that permits to identify and analyse the emissive species (atoms, molecules and ions) present in the plasma. It permits to follow the evolution of the emission intensity of these species. The principle is briefly described as follow [21]: when specie is excited in a special high energy level E_j, it de-excites in other lower energy level E_i with a certain probability A_{ji}. The difference of energy is translated in a photon emission with energy $h\upsilon_{ji} = E_j - E_i = \Delta E_{ji}$ and this energy difference corresponds to a certain wavelength $\lambda_{ji} = \frac{hc}{\Delta E_{ji}}$. This wavelength is specific only to that specie. So, by using a specific table, all the emissive species present in the plasma could be identified. The following relation gives the emission intensity of this specie $I_{ji} = C_{ji} A_{ji} n_j h\upsilon_{ji}$ Where C_{ji} and n_j are

respectively the apparatus constant and the density of the specie and h the Planck constant. By measuring this intensity as a function of the plasma parameters, the evolution of the relative quantity of the species could be followed. The **Erreur ! Source du renvoi introuvable.Erreur ! Source du renvoi introuvable.** illustrates the evolution of the CN and C_2 radical's optical emission intensities with and without presence of silicon substrate, as a function of the CH4 percentage in the gas mixture. The microwave power is fixed at 1000 W, the gas pressure at 50 mbar and the total gas flow rate at 50 sccm.

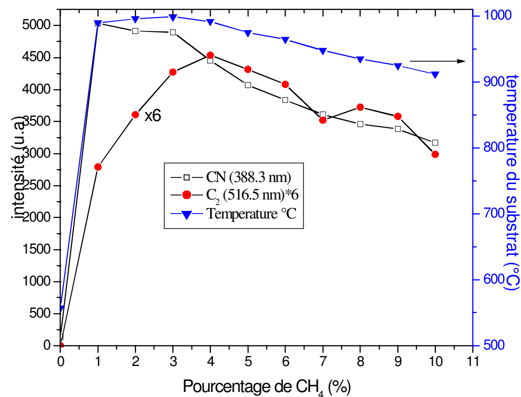

a)

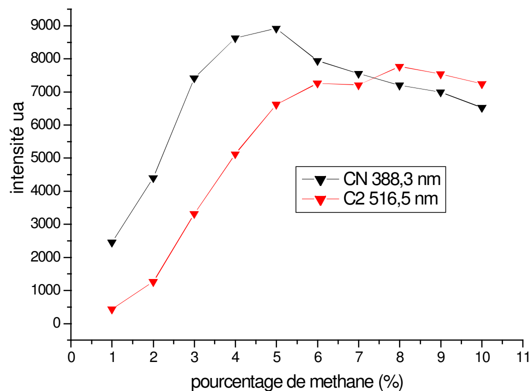

b)

Figure 3. Evolution of CN and C_2 radicals OES emission intensities with and without silicon substrate under the plasma, as a function of the methane percentage in the gas mixture. The microwave power is fixed at 1000 W, the pressure at 50 mbar and the total flow rate at 50 sccm

The figure shows that the evolution curves of the emission intensity of CN and C_2 are almost the same. They intensities increase until 4 % CH_4 and decrease slightly beyond this value. These results indicate also that the reactivity of the gas mixture in the N_2/CH_4 discharge is more important for a percentage of CH_4 around to 4%. Without silicon substrate, the intensity emitted by the radical C_2 is 6 times much higher than the case where there was the silicon substrate. No continuous film deposition was possible on the molybdenum plate or WC-Co substrate. Only carbon powder formation was observed on such materials. This carbon is related to the high amount of C_2 observed by OES in this case compared to the case where there was a silicon substrate under the plasma. When there is no film deposition, the emission intensity of C_2 is as strong as that of CN, whereas when film deposition occurs, the emission of CN is 6 times greater than that of C_2. This means that during the films synthesis, C_2 or CH_x radicals are likely the principals responsible for the deposition. They are so consumed during the film deposition. Great parts of the observed CN are products of the carbon etching by atomic nitrogen. The CN radicals probably don't contribute directly to the deposition while C_2 represent species involved in the deposition.

3. - Characterization of the films morphology

The general morphology and topography of the films are observed by SEM and AFM. To study the crystallites morphology and structure, observations on top view of the films fragments are carried out by TEM. A typical film is observed by SEM, AFM and TEM and the micrographs are presented on **Erreur ! Source du renvoi introuvable.**.

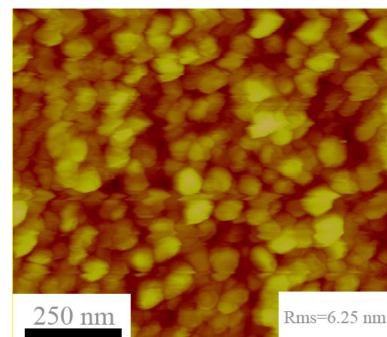

a)

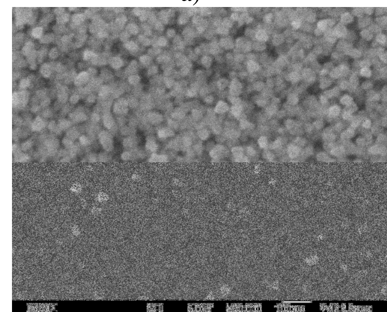

b)

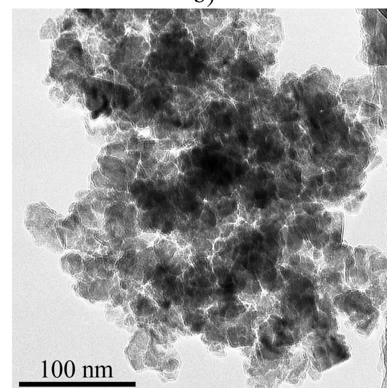

c)

Figure 4. Micrographs obtained by a) AFM and b) SEM on a film deposited at 800 W, 50 mbar, 50 sccm, and c) TEM on a film deposited at 1000 W, 50 mbar, 50 sccm

The films obtained by continuous MPACVD are nanocrystalline and the grains size varies between 20 to 70 nm. The roughness of the films observed by AFM is a function of the average grain size of the crystallites and the Rms is around 6 nm. The morphology of our films as observed by SEM, AFM and TEM differ from those that are observed by others authors. In our case, hexagonal rods with a grain size larger than 1 µm are not obtained as observed in literature [12, 22- 23]. The films are constitutes of crystallites with various grain sizes and forms. The crystallites present square, triangle and hexagonal faces that proves that the films are certainly constituted of cubic, tetrahedral and hexagonal crystallites.

4. – Films structure characterization

The atomic distances (d_{hkl}) have been calculated by using the XRD angles and compared with those of the Joint Committee on Powder Diffraction Standards (JCPDS) database. The comparison has been done with the dh_{kl} files in the JCPDS database of all the compounds formed by combination of carbon, silicon and nitrogen.

All the peaks on all the DRX spectra of the films realized while varying the percentage of methane have been identified and listed in **Erreur ! Source du renvoi introuvable.**.

Table 1. d_{hkl} obtained from the XRD peaks of the films realized by varying the percentage of methane in the gas, compared with d_{hkl} from the JCPDS database

Experiment						JCPDS					
						βC_3N_4 (N°50-1250)		C_3N_4 cubic (N°1-78-1693)		SiCN (N°1-74-2309)	
dhkl (Å)	2%	4%	8%	12%	14%	hkl	d(Å)	hkl	d(Å)	hkl	d(Å)
						100	5.565				
								100	3.43		
						110	3.213				
2.72	*	*	*	*	*	200	2.783				
2.51	0	*	*	*	*					111	2.52
								110	2.42538		
						101	2.259				
										200	2.18
						210	2.103				
1.97	*	*	*	*	*			111	1.98031		
1.95	*	*	0	*	0	111	1.95				
1.90	*	*	*	*	*	300	1.855				
1.68	*	*	*	*	*			200	1.715		
1.65	*	0	*	*	*						
1.63	*	*	*	*	*	211	1.598				
1.50	*	*	*	*	*	310	1.543	210	1.53391	220	1.54
1.42	*	*	*	*	*	301	1.481				
1.40	*	*	*	*	*			211	1.40029		
						221	1.345				
										311	1.31
1.25	*	*	*	*	*	320	1.277			222	1.26
						002	1.229				
								220	1.21269		
								221	1.14333		
						321	1.133				
						202	1.125				
1.1	*	0	0	*	*	411	1.089			400	1.09
1.00	*	*	*	*	*						
0.95	*	*	*	*	*						
0.91	*	*	*	*	*						
0.90	*	*	*	*	*						
0.84	*	*	0	*	*						

After the comparison, structures that correspond most closely to those which are present in our films are: β-C_3N_4 (JPCDS file n°50-1250), c-C_3N_4 (JPCDS n° 1-078-1693) and c-SiCN (JPCDS n° 1-074-2309). In **Erreur ! Source du renvoi introuvable.**, some d_{hkl} of the phases are missing, and also other experimental d_{hkl} do not match with any phase of the JCPDS database. For example, while the majority of d_{hkl} corresponding to β-C_3N_4 seem to be emerging, the d_{hkl} corresponding to the plan (100), (110), (101), (210) plan are absent in the table. The lack of some d_{hkl} has also been observed by other authors [24]. It could be explained by a texture apparition or a variation of the

Copyright© 2014 Revue CAMES SAI

lattice parameters due to constraint in the films or by a lack of enough quantity of material necessary for the analysis.
To complete our investigation on the structural characterization and the identification of phases, SAED has also been used. The **Erreur ! Source du renvoi introuvable.** shows some patterns for film deposited at different methane percentage.

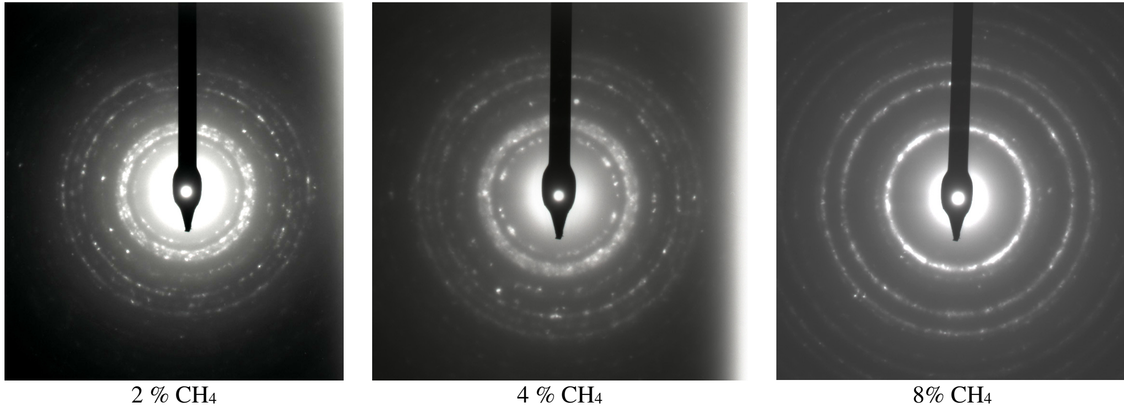

Figure 5. SAED patterns for films realize at different methane percentage. The dhkl have been calculated with the rings obtained on the SAED patterns. The obtained dhkl are listed in the Erreur ! Source du renvoi introuvable. **and compared to the JCPDS database**

Table 2. dhkl obtained from the SAED rings of the films realized by varying the percentage of methane in the gas, compared with dhkl from the JCPDS database

Experiment		**JCPDS**					
		βC_3N_4 (N°50-1250)		**C_3N_4 cubic (N° 1-078-1693)**		**SiCN (N°1-074-2309)**	
N°	d $_{\pm 5\%}$ (Å)	hkl	d(Å)	hkl	d(Å)	hkl	d(Å)
1		100	5.565				
2				100	3.43		
3	3.20	110	3.213				
4	2.76	200	2.783				
5	2.54					111	2.52
6	2.42			110	2.42538		
7		101	2.259				
8						200	2.18
9		210	2.103				
10	1.98	111	1.95	111	1.98031		
11	1.87	300	1.855				
12	1.68			200	1.715		
13		211	1.598				
14	1.57	310	1.543	210	1.53391	220	1.54
15	1.44	301	1.481	211	1.40029		
16	1.34	221	1.345			311	1.31
17				220	1.21269		
18		320	1.277			222	1.26
19		002	1.229				
20	1.13	321	1.133	221	1.14333		
21		202	1.125				
22		411	1.089			400	1.09
23	1.03						
24	0.89						
25	0.74						

Most of the obtained rings could correspond to the same peaks obtained by XRD, but some rings are absent in the SAED pattern. For instant, the (110) of β-C_3N_4 and (311) of c-SiCN for example have been observed by SAED but not by XRD.

The combination of the XRD and SAED results allow the phase identification process. In order to know if the lack of some rings in the SAED pattern and peaks in the XRD spectrum is due to a beginning of texture, bright field and dark field top view TEM images and SAED have been performed while changing the

observation angle on a typical sample deposited at 4% CH_4, 1000 W, 50 mbar, 50 sccm. The **Erreur ! Source du renvoi introuvable.**-a corresponds to a bright filed TEM micrograph obtained at 0, and the **Erreur ! Source du renvoi introuvable.**-b, 6-c and 6-d correspond respectively to a dark field TEM micrographs realised at -20°, 20° and -35°.

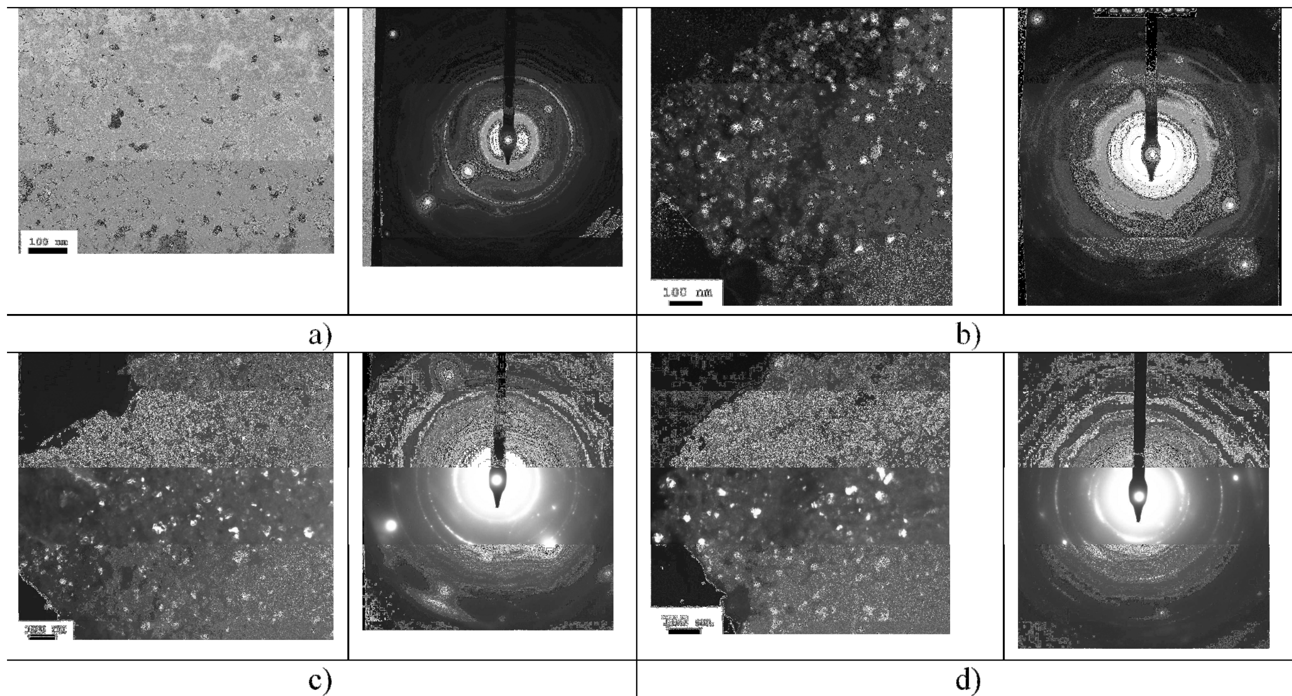

Figure 6. SAED and TEM micrographs realized on a silicon carbon nitride film observed under different angles on top view in bright field (a): angle = 0 and dark field (b): angle= -20 °, c): angle= 20° and d): angle=35

When the observation angle is changed, the diffracting crystallites respecting the Braggs law change thus the SAED shows more or less d_{hkl}. The **Erreur ! Source du renvoi introuvable.** also shows that the dark field micrographs differ from an angle to another one. Thus the observed crystallites on the dark field TEM micrograph are those contributing to the diffraction pattern at each observation angle. The calculated d_{hkl} from the diffraction rings obtained on these SAED patterns are summarized in **Erreur ! Source du renvoi introuvable.**. For each experimental d_{hkl}, the observation angles is noted in the left column. The experimental d_{hkl} is compared to those of the JCPDS database.

Table 3. Comparison between experimental d_{hkl} obtained from SAED patterns observed trough different angles on the same sample (a=0°, b= -20°, c=20° and d= -35°) and JCPDS database of β-C_3N_4, cubic-C_3N_4 and SiCN

Angles	Experimental d_{hkl}	βC_3N_4 JCPDS N°50-1250		Cubic-C_3N_4 JCPDS N° 1-078-1693		SiCN JCPDS N°1-074-2309	
	d ±5% (Å)	**hkl**	**d(Å)**	**hkl**	**d(Å)**	**hkl**	**d(Å)**
		100	5.57				
				100	3.43		
a, b	3.20	110	3.21				
		200	2.78				
a, b, c, d	2.54					111	2.52
				110	2.43		
		101	2.26				
a, d	2.20					200	2.18
		210	2.10				
a,	1.91	111	1.95	111	1.98		
		300	1.86				
				200	1.72		
		211	1.60				
a, b, c, d	1.55	310	1.54	210	1.53	220	1.54
a,	1.42	301	1.48	211	1.40		
a, b, c	1.31	221	1.35			311	1.31
				220	1.21		
b, d		320	1.28			222	1.26

		002	1.23				
		321	1.13	221	1.14		
		202	1.13				
	1.10	411	1.09			400	1.09
a, b, c, d	1.01						
a, b, c, d	0.90						
a, b, d	0.84						

As shown in this table 3, some observation angles do not permit the observation of some diffraction rings. Most of the d_{hkl} obtained by XRD have been observed and supplementary d_{hkl} have also been determined. These results are complementary of XRD ones and prove that, the film present a beginning of texture and contain probably the β-C_3N_4, c-C_3N_4 and c-SiCN phases.

5. – Films chemical composition and bonding structure characterization

The film surface composition is analysed by XPS. These analyses have been done without removing the natural oxidation that occurs after the film deposition and exposed to atmosphere air. Film surface is cleaned by argon ions sputtering because, in our case, this bombardment promotes the formation of supplementary carbon bonds in the film, due to a preferential sputtering of the obtained elements. Indeed, the bombardment of the film by argon ions modifies the bonding structure and increases the carbon bonds. So in this study all the films are observed without any surface bombardment. Consequently the oxygen percentage has been substrates to the calculation of the films composition. The silicon coming from the Si-Si bonds have also been subtracted because, this part probably comes from the silicon substrate without any recombination with the other elements. Indeed, the film is thin and porous, thus the X-ray can reach the silicon substrate and analyse the Si-Si bonds. The **Erreur ! Source du renvoi introuvable.** shows the a) C1s, b) N1s, c) Si2p and d) O1s XPS spectrum realised on a SiCN film deposited at 4% CH_4, 800 W, 50 mbar, 50 sccm.

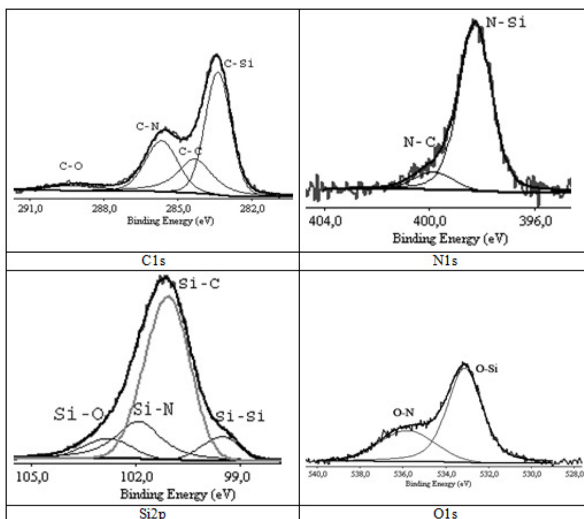

Figure 7. a) C1s, b) N1s, c) Si2p and d) O1s XPS spectra obtained by XPS on a film deposited in continuous mode at 4 % CH4, 800 W, 50 mbar, 50 sccm

In the Si2p line, the peaks situated at 99.4, 100.9, 101.9 and 102.6 eV are respectively attributed to Si-Si, Si-C, Si-N, and Si-O bonds. The Si is mostly bonded to C than N. Our results don't confirm the observations of Chen et al [25] who show that the silicon is preferentially bonded to N. From the C1s line, the carbon bonds C-Si, C-C, C-N and C-O could be positioned respectively at 283.4, 284.3, 285.7 and 289.16 eV. In the N1s line, the nitrogen bonds N-Si and N-C are situated respectively at 398.1 and 399.4 eV. In the O1s line, oxygen bonds are located at 533.2 and 534.6 eV corresponding to O-Si and O-N bonds. These different bonds observed in the present work, have also been observed by other authors [26, 27] in the case of SiCN and CNx films. The presence of oxygen is due to an oxidation after air exposure. The presence of silicon bonding is due to the plasma etching of the substrate during the deposition process. The growth mechanisms have been approached in a previews work [28]. Briefly the radicals coming from the plasma volume (N, H…) etch the silicon substrate and recombine with carbon and nitrogen in volume before contributing to the growth of the film.

4. Conclusion

Nanocrystalline CN_x and SiCN films are synthesised by continuous MPACVD in CH_4/N_2 gas mixture on silicon substrates. The films are characterized by a combination of different techniques. SEM, TEM and AFM characterizations show that the films are nanocrystalline. The grain size varies from 20 to 70 nm and the film surface Rms is around 6 nm. In spite of the lack of some XRD peaks or some diffraction rings in the SAED patterns due to the texture effect, we can conclude that probably the thin films which have been synthesised contain a mixture of β-C_3N_4, c-C_3N_4 and c-SiCN phases. The hypothetic β-C_3N_4 phase is found to be embedded in other crystalline phases as compared to other authors' works where it is found to be embedded generally in amorphous CN_x phase.

Acknowledgements

This project was supported by the "Fonds National de la Recherche" of Luxembourg. This work is also partly supported by the "Ministère délégué à l'Enseignement Supérieur et à la Recherche" of France and the Ivory Coast Government. The authors wish to thank J. Ghanbaja, P. Miska, and J. P. Emeraux from Nancy University for TEM, AFM and XRD analyses respectively.

Copyright© 2014 Revue CAMES SAI

REFERENCES

[1] A. Y. Liu, M. L. Cohen, “Prediction of new low compressibility solids,” Science, Vol. 245, Issue 4920, 1989, pp. 841 - 842.

[2] E. Bertran, F. J. Pino, G. Viera, J. L. Andujar, “Hard coatings for mechanical applications,” Vacuum, Vol. 64, Issues 3-4, 2002, pp. 181 - 90.

[3] K. J. Boyd, D. Marton, J. W. Rabalais, Y. Lifshitz “Semiquantitative subplantation model for low energy ion interactions with surfaces. II. Ion beam deposition of carbon and carbon nitride,” Journal of vacuum Science and Technology A, Vol. 16, 1998, pp. 455 - 462

[4] H. Riascos, J. Neidhardt, G. Z. Radnoczi, J. Emmerlich, F. Zambrano, L. Hultman, P. Prieto, “Structure and properties of pulsed-laser deposited carbon nitride thin films,” Thin Solid Films, Vol. 497, Issues 1-2, 2006, pp. 1 - 6.

[5] X. W. Liu, J. H. Lin, C. H. Tseng, H. C. Shih, “Optical and structural properties of the amorphous carbon nitride by ECR-plasma,” Materials Chemistry and Physics, Vol. 72, Issue 2, 2001, pp. 258 - 263.

[6] W. C. Chang, M. K. Fung, I. Bello, C. S. Lee, S. T. Lee, “Nitrogenated amorphous carbon films synthesized by electron cyclotron resonance plasma enhanced chemical vapor deposition,” Diamond and Related Materials, Vol. 8, Issues 8-9, 1999, pp. 1732 - 1736.

[7] G. Dinescu, E. Aldea, G. Musa, M. C. M. Van de Sanden, A. de Graaf, C. Ghica, M. Gartner, A. Andrei, “Characterization of carbon nitride thin-films deposited by a combined RF and DC plasma beam,” Thin Solid Films, Vol. 325, Issues 1-2, 1998, pp. 123 - 129.

[8] J. Hao, T. Xu, W. Liu, “Preparation and characterization of hydrogenated carbon nitride films synthesized by dual DC-RF plasma system,” Materials Science and Engineering: A, Vol. 408, Issues 1-2, 2005, pp. 297 - 302.

[9] D. K. Lee, D. H. Kang, H. Y. Lee, J. J. Lee, “Properties of carbon nitride films produced by an inductively coupled plasma chemical vapor deposition,” Surfaces and Coatings Technology, Vol. 188-189, 2004, pp. 440 - 445.

[10] H. Gruger, D. Selbmann, E. Wolf, A. Leonhardt, “Influence of RF plasma properties on the deposited PACVD CN_x layers,” Surface and Coatings Thechnology, Vol. 97, Issues 1-3, 1997, pp. 109 - 113.

[11] Y. P. Zhang, Y. S. Gu, “Effect of silicon impurity on carbon nitride films prepared by microwave plasma chemical vapor deposition,” Materials Science and Engineering: B, Vol. 85, Issue 1, 2001, pp. 38 - 42.

[12] Y. Sakamoto, M. Takaya, “Download Fabrication of nitrogen included carbon materials using microwave plasma CVD,” Surface and Coatings Technology, Vol. 169-170, 2003, pp. 321 - 323.

[13] S. Matsumoto, E. Q. Xie, F. Izumi, “On the validity of the formation of crystalline carbon nitrides C_3N_4,” Diamond and Related Materials, Vol. 8, Issue 7, 1999, pp. 1175 - 1182.

[14] E. Kroke, M. Schwarz, “Novel group 14 nitrides,” Coordination Chemistry Reviews, Vol. 248, Issues 5-6, 2004, pp. 493 - 532.

[15] S. Muhl, J. M. Mendez, “A review of the preparation of carbon nitride films,” Diamond and Related Materials, Vol. 8, Issue 10, 1999, pp. 1809 - 1830.

[16] T. Lamara, M. Belmahi, J. Bougdira, F. Benedic, G. Henrion, M. Remy, “Diamond thin film growth by pulsed microwave plasma at high power density in a CH_4–H_2 gas mixture,” Surfaces and Coatings Technology, Vol. 174-175, 2003, pp. 784 - 789.

[17] H. Chatei, J. Bougdira, M. Rémy, P. Alnot, C. Bruch, J. K. Krüger, “Effect of nitrogen concentration on plasma reactivity and diamond growth in a H_2-CH_4-N_2 microwave discharge,” Diamond and Related Materials, Vol. 6, Issue 1, 1997, pp. 107 - 119.

[18] T. Malkow, “Critical observations in the research of carbon nitride,” Materials Science and Engineering A, Vol. 302, Issue 2, 2001, pp. 311 - 324.

[19] P. Kouakou, V. Brien, M. B. Assouar, V. Hody, M. Belmahi, H. N. Migeon, J. Bougdira, “Preliminary synthesis of carbon nitride thin films by N_2/CH_4 microwave plasma assisted chemical vapour deposition: characterisation of the discharge and the obtained films ,” Plasma Processes and Polymers , Vol. 4, 2007, pp. 210 - 214.

[20] M. Gajdos, A. Eichler, J. Hafner, “Ab initio density functional study of O on the Ag(0 0 1) surface,” Surface Science, Vol. 531, Issue 3, 2003, pp. 272 - 286.

[21] A. Richard, “Plasma plasmas,” SFV, Société Française du vide, 1995.

[22] Y. S. Gu, Y. P. Zhang, Z. J. Duan, X. R. Chang, Z. Z. Tian, N. X. Chen, C. Dong, D. X. Shi, X. F. Zhang, L. Yuan, “Criystalline β-C_3N_4 synthesized by MPCVD,” Journal of Materials Science, Vol. 34, Issue 12, 1999, pp. 3117 - 3125.

[23] Y. P. Zhang, Y. S. Gu, X. R. Chang, Z. Z. Tian, D. X. Shi, X. F. Zhang, “On the structure and composition of crystalline carbon nitride films synthesized by microwave plasma chemical vapor deposition,” Materials Science and Engineering: B, Vol. 78, 2000, pp. 11 - 15.

[24] K. M. Yu, M. L. Cohen, E. E. Haller, W. L. Hasen, A. Y. Liu, I. C. Wu, “Observation of crystalline C_3N_4,” Physical review B, Vol. 49, Issue 7, 1994, pp. 5034 - 5037.

[25] C. W. Chen, C. C. Huang, Y. Y. Lin, L. C. Chen, K. H. Chen, “ The affinity of Si-N and Si-C bonding in amorphous silicon carbon nitride (a-SiCN) thin films,” Diamond and Related Materials, Vol. 14, Issues 3-7, 2005, pp. 1126 - 1130.

[26] E. Xie, Z. Ma, H. Lin, Z. Zhang, D. He, “Preparation and characterization of SiCN films,” Coordination Chemistry Reviews, Vol. 23, Issues 1-2, 2003, pp. 151 - 156.

[27] H. K. Woo, Y. Zhang, S. T. Lee, C. S. Lee, Y. W. Lain, K. W. Wong, “Preparation and crystalline carbon nitride films on silicon substrate by chemical vapor deposition,” Diamond and Related Materials, Vol. 6, Issue 5-7, 1997, pp. 635 - 639.

[28] P. Kouakou, M. Belmahi, V. Brien, V. Hody, H. N. Migeon, J. Bougdira, “Role of silicon on the growth

mechanisms of CNx and SiCN thin films by N_2/CH_4 microwave plasma assisted chemical vapour deposition," Surface and Coatings Technology, Vol. 203, 2008, pp. 277 - 283.